

# SAM-SP: Self-Prompting Makes SAM Great Again

Chunpeng Zhou\*, Kangjie Ning\*, Qianqian Shen, Sheng Zhou, Zhi Yu, Haishuai Wang<sup>†</sup>

Zhejiang University, China  
zhoucp@zju.edu.cn, haishuai.wang@gmail.com

## Abstract

The recently introduced Segment Anything Model (SAM), a Visual Foundation Model (VFM), has demonstrated impressive capabilities in zero-shot segmentation tasks across diverse natural image datasets. Despite its success, SAM encounters noticeably performance degradation when applied to specific domains, such as medical images. Current efforts to address this issue have involved fine-tuning strategies, intended to bolster the generalizability of the vanilla SAM. However, these approaches still predominantly necessitate the utilization of domain specific expert-level prompts during the evaluation phase, which severely constrains the model's practicality. To overcome this limitation, we introduce a novel self-prompting based fine-tuning approach, called SAM-SP, tailored for extending the vanilla SAM model. Specifically, SAM-SP leverages the output from the previous iteration of the model itself as prompts to guide subsequent iteration of the model. This self-prompting module endeavors to learn how to generate useful prompts autonomously and alleviates the dependence on expert prompts during the evaluation phase, significantly broadening SAM's applicability. Additionally, we integrate a self-distillation module to enhance the self-prompting process further. Extensive experiments across various domain specific datasets validate the effectiveness of the proposed SAM-SP. Our SAM-SP not only alleviates the reliance on expert prompts but also exhibits superior segmentation performance comparing to the state-of-the-art task-specific segmentation approaches, the vanilla SAM, and SAM-based approaches.

## Introduction

Recent years have witnessed the remarkable evolution of Foundation Models, deemed as a generalized AI paradigm (Bommasani et al. 2021). These Foundation models have demonstrated exceptional performance across various real-world downstream tasks with minimal human intervention. Examples include the renowned ChatGPT (Ouyang et al. 2022), GPT-4 (Achiam et al. 2023), CLIP (Radford et al. 2021), and BLIP (Li et al. 2022), etc., all of which achieved remarkable success with minimal human intervention. However, these models were not specifically engineered for image segmentation (Minaee et al. 2021), an important computer vision task. The recent introduced Segment Anything

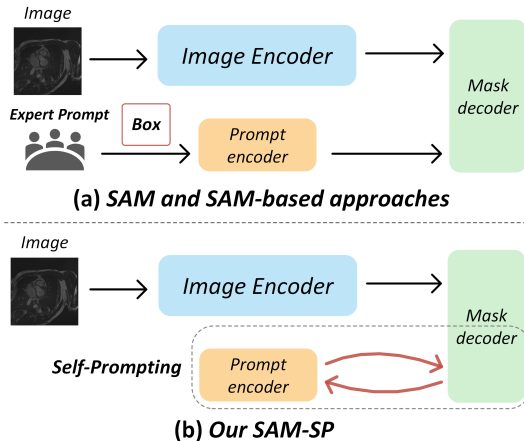


Figure 1: The illustration of our model. (a) SAM and SAM-based approaches both rely on the expert prompts during inference. (b) Our SAM-SP build a self-prompting module and do not rely on the expert prompts during inference.

Model (Kirillov et al. 2023) (SAM), a Foundation Visual Model for image segmentation, aims to address a range of downstream segmentation tasks. Trained on the extensive SA-1B dataset (Kirillov et al. 2023), which encompasses over 1 billion masks from 11 million images, SAM generates high-quality object masks and has demonstrated distinguished capabilities across diverse natural image datasets. Notably, SAM supports the flexible prompts from users, including point, box, and mask prompts. The zero-shot performance of SAM is impressive, often competitive with or even superior to prior fully supervised segmentation approaches (Kirillov et al. 2023) across various natural datasets.

Given these advancements, there is a natural inclination to apply SAM to specific domains, such as medical images (Litjens et al. 2017; Hesamian et al. 2019), remote sensing images (Jiang et al. 2022; Shafique et al. 2022), and road damage images (Yang et al. 2019; Fan et al. 2019), etc. For instance, precise medical image segmentation is crucial for various clinical applications, including disease diagnosis, treatment planning, and disease progression monitoring. However, significant domain gaps exist between natural and

\*These authors contributed equally.

<sup>†</sup>Corresponding Author

medical images, including blurred boundaries and low contrast in medical images. Experimental results from previous studies (Ji et al. 2023; He et al. 2023; Zhou et al. 2023b; Ma et al. 2024; Mattjie et al. 2023; Ning, Zhou, and Yu 2023; Ahmadi et al. 2023) have indicated that directly applying SAM to these domains usually leads to noticeable performance degradation, with SAM significantly underperforming compared to traditional task-specific medical image segmentation approaches like U-net (Ronneberger, Fischer, and Brox 2015) and U-net++ (Zhou et al. 2020).

To address these challenges and broaden SAM’s application range, recent approaches (Ma et al. 2024; Wu et al. 2023) attempt to fine-tuning the vanilla SAM model with domain-specific data. For example, MedSAM (Ma et al. 2024) utilizes a simple fine-tuning method on a medical image dataset to adapt SAM to medical image segmentation tasks, while SAM-Med2D (Cheng et al. 2023) employs adaptation techniques (Chen et al. 2022) on the image encoder of SAM. Despite these improved performance in specific domains compared to the vanilla SAM, they still heavily rely on the precision of provided prompts during inference (Wu et al. 2023) as shown in Fig 1. In fact, their performance may degrade to the level of the vanilla SAM if the provided prompts are not sufficiently accurate (Wu et al. 2023). Unfortunately, in contrast to natural images, the availability of precise prompts is difficult for specific domains, such as medical images, which heavily rely on expert domain knowledge. This limitation may hinder the widespread application of SAM. To abbreviate the need for expert prompts, we pose a question: *can we make SAM perform well without any user prompts during inference?* Inspired by the training strategy of SAM, where SA-1B (the training dataset of SAM) only includes automatically generated masks by SAM itself as ground truth (Kirillov et al. 2023), we attempt to produce reliable prompts independently without relying on expert prompts during inference.

Consequently, we introduce a SAM-based segmentation framework with a novel proposed Self-Prompting strategy, called **SAM-SP**, allowing the model to produce prompts autonomously, eliminating the need for user prompts during inference. SAM-SP builds upon the basic framework of the vanilla SAM, which encodes the input image using a ViT (Dosovitskiy et al. 2020) based image encoder. Furthermore, we employ a low-rank-based finetuning strategy (LoRA) (Hu et al. 2021), which allows SAM to better adapt to downstream tasks and makes training more efficient compared to full fine-tuning. And then the mask decoder utilize the image embeddings obtained by the image encoder to produce initial predictions. To alleviate the dependence on expert prompts during inference, we incorporate a Self-Prompting module to generate prompts by the model itself. Specifically, the Self-Prompting module utilizes the first predictions to generate prompts for guiding the subsequent iteration of the model. In next iteration, the prompt encoder encodes the generated prompts into prompting embeddings, which are then fed to the mask decoder to obtain refined predictions. Though the supervised segmentation signals during training, SAM-SP learns to produce reliable and meaningful prompts by itself. Additionally, we utilize a segmentation

based self-distillation module to further enhance the training of the self-prompting module. We leverage the later predictions as a teacher to guide previous predictions in our self-distillation module. SAM-SP gains mutual benefits from the self-distillation module. On the one hand, the final prediction provides additional supervision signals to guide the previous prediction of SAM-SP. On the other hand, the previous predictions provide more accurate prompts for subsequent predictions. We conduct extensive experiments on diverse and publicly available datasets. The results indicate that our proposed SAM-SP achieves satisfactory performance without user prompts, compared to state-of-the-art task-specific segmentation approaches, the vanilla SAM, and SAM-based approaches.

Our contributions in this paper are summarized as follows: (i) We highlight the significance of diminishing reliance on expert prompts when deploying a visual foundation model in specific domains, such as the Segment Anything Model (SAM) in medical images. (ii) We introduce SAM-SP, a SAM-based framework which incorporates a novel self-prompting module, extending the vanilla SAM to explore its capability across various downstream tasks, without relying on expert prompts during inference. We further integrate a self-distillation module to enhance the self-prompting module. (iii) We build and release a novel and challenging segmentation dataset Seg-GPR for SAM, aiming for subgrade distress segmentation and collected by a 3-D ground penetrating radar. (iv) We conduct comprehensive evaluations of the proposed SAM-SP on diverse and publicly available datasets, which demonstrate superior performance without using any user prompts, compared to state-of-the-art task-specific segmentation approaches, the vanilla SAM, and SAM-based approaches.

## Related Work

### Vision Foundation Model (LVM)

Recent Large Language Model (Zhao et al. 2023a) like ChatGPT (Ouyang et al. 2022), GPT-4 (Achiam et al. 2023) have demonstrated exceptional performance in various NLP tasks. Similarly, Vision Foundation Models (LVM) have received huge attention. For example, CLIP (Radford et al. 2021) utilizes a contrastive learning strategy trained on 400 million image-text pairs collected from the internet, achieving excellent performance in a wide variety of downstream tasks. Inspired by pre-training strategies in NLP (Kenton and Toutanova 2019), MAE (He et al. 2022) employs an asymmetric encoder-decoder structure, aiming to reconstruct original images from random subsets of patches. Experimental results of MAE demonstrate the excellent transfer performance in downstream tasks. In another line, DALL-E (Ramesh et al. 2021) is built based on a large autoregressive transformer, designed to generate images from textual descriptions. GPT-4 with Vision (GPT-4V) extends the capabilities of GPT-4 by incorporating visual modalities, enabling users to analyze image inputs (Achiam et al. 2023). Distinct from previous VFM, Segment Anything Model (Kirillov et al. 2023) (SAM) is the first VFM, specifically designed for segmentation tasks. Trained on the large SA-1B

dataset, SAM demonstrates exceptional zero-shot segmentation performance in natural images.

## SAM and SAM-based approaches

To extend SAM’s applicability to specialized domains, recent approaches have aimed to improve the vanilla SAM. Notably, MedSAM (Ma et al. 2024) is the first attempt to extend SAM to medical images, employing a simple fine-tuning method with a large collected medical image dataset. SAM-Med2D (Cheng et al. 2023) and SAM-Adapter (Chen et al. 2023) both utilize adaptation techniques (Chen et al. 2022) on the image encoder of SAM, instead of the simple fine-tuning. The Medical SAM Adapter (Wu et al. 2023) (Med-SA) introduces Space-Depth Transpose (SD-Trans) and Hyper-Prompting Adapter (HyP-Adpt) modules to achieve prompt-conditioned adaptation for medical image segmentation. SAMed (Zhang and Liu 2023) applies a LoRA-based (Hu et al. 2021) fine-tuning strategy to SAM’s image encoder, jointly fine-tuning it together with the prompt encoder and mask decoder of SAM without user prompts. SAMUS (Lin et al. 2023) extends SAM by incorporating a parallel CNN branch, aiming to inject local features into the image encoder of SAM through cross-branch attention. The adapter technique (Chen et al. 2022) is also used in SAMUS. Though these SAM-based approaches improve the generalization abilities of SAM, they predominantly ignore the difficulties of precise prompts in specific domains, particularly in medical datasets. Consequently, we proposed a new framework SAM-SP which aims to produce prompts automatically during inference. Additionally, we highlight the difference between our approach and the related work by Wu, Zhang, and Elbatel, which introduces a simple logistic regression as the Self-Prompt Unit. The unit predicts a coarse mask from the image embeddings, and then uses it to obtain the bounding box as the prompt. In contrast, our SAM-SP learns to generate the prompts from the output of the SAM mask decoder, resulting in more precise prompts than those produced by simple logistic regression. Furthermore, we employ LoRA-based fine-tuning for better adaptation to downstream tasks, whereas only the logistic regression component is trainable in their framework (Wu, Zhang, and Elbatel 2023), which may lead to limited generalization ability.

## Recap of the Segment Anything Model

Before delving into the details of SAM-SP, we first review the basic framework of the first visual segmentation foundation model Segment Anything Model (SAM) (Kirillov et al. 2023), containing three main components: an image encoder, a prompt encoder, and a lightweight mask decoder. The image Encoder leverages an MAE (He et al. 2022) pre-trained Vision Transformer (ViT) (Dosovitskiy et al. 2020) to encoder the input images. The prompt encoder is designed to encoder the user-provided prompts, which supports multiple types of prompts, including both sparse (points, boxes) and dense (masks) prompts. Then, the mask decoder combines the image and prompt embeddings to predict the target mask. In this paper, we use  $E(\cdot)$ ,  $P(\cdot)$  and  $M(\cdot)$  to denote

image encoder, prompt encoder, and mask decoder, respectively. As discussed above, the vanilla SAM struggles in specific domains and relies on the domain specific expert-level prompts during inference.

## Methodology

### Overview of Our Method

As illustrated in Figure 2, our proposed SAM-SP aims to enhance the segmentation capability of SAM in specific domains while reducing the reliance on expert prompts. SAM-SP is an end-to-end framework built on the vanilla SAM, containing three additional modules: LoRA-based fine-tuning, the Self-Prompt module and the Self-Distillation module.

### LoRA-based Fine-tuning

As discussed above, significant domain gaps usually arise between downstream datasets (e.g. medical images) and natural images, for which the vanilla SAM is engineered. To mitigate these gaps and improve the generalization abilities of SAM, fine-tuning has been widely adopted in previous works (Ma et al. 2024; Cheng et al. 2023; Wu et al. 2023; Zhang and Liu 2023; Lin et al. 2023). Instead of fine-tuning the all parameters of SAM, we freeze the image encoder, and only fine-tune the prompt encoder and mask decoder to minimize computational costs, given that the image encoder dominates the majority (more than 95%) computational overhead in SAM. To further enhance the quality of image embeddings from the image encoder, we employ a low-rank-based fine-tuning strategy (LoRA) (Hu et al. 2021), which approximates the low rank update of the parameters in the image encoder. LoRA enables SAM to adapt effectively to downstream tasks, while maintaining training efficiency compared to full fine-tuning. Additionally, LoRA merges the trainable matrices with the frozen weights when deployed, introducing no additional inference latency. For a pre-trained weight matrix  $\mathbf{W} \in \mathbb{R}^{d \times k}$  in the SAM image encoder, we suppose its update as follows:  $\hat{\mathbf{W}} = \mathbf{W} + \Delta\mathbf{W} = \mathbf{W} + \mathbf{B}\mathbf{A}$ , where  $\hat{\mathbf{W}} \in \mathbb{R}^{d \times k}$  denotes the updated weight matrix, and a low-rank decomposition  $\Delta\mathbf{W} = \mathbf{B}\mathbf{A}$ ,  $\mathbf{A} \in \mathbb{R}^{r \times d}$ ,  $\mathbf{B} \in \mathbb{R}^{d \times r}$  models this weight update. We set 4 as the default rank of the low-rank decomposition in our implementation.

### Self-Prompting Module

As depicted in Fig 2, we introduce a Plug-and-Play Self-Prompting module to alleviate the need of expert prompts. Previous works typically simulate user prompt according the expert annotations during the training stage. For example, MedSAM (Ma et al. 2024), Med-SA (Wu et al. 2023) and SAM-Med2D (Cheng et al. 2023) all employ the ground truth prompts during both training and evaluation. However, this may lead to models becoming overly reliant on provided prompts. To reduce this reliance and achieve training-test matching, we do not use any user prompts during both training and evaluation. The prompt encoder in SAM can work without any prompt input, and will update a default embedding during training (Kirillov et al. 2023). Formally, given

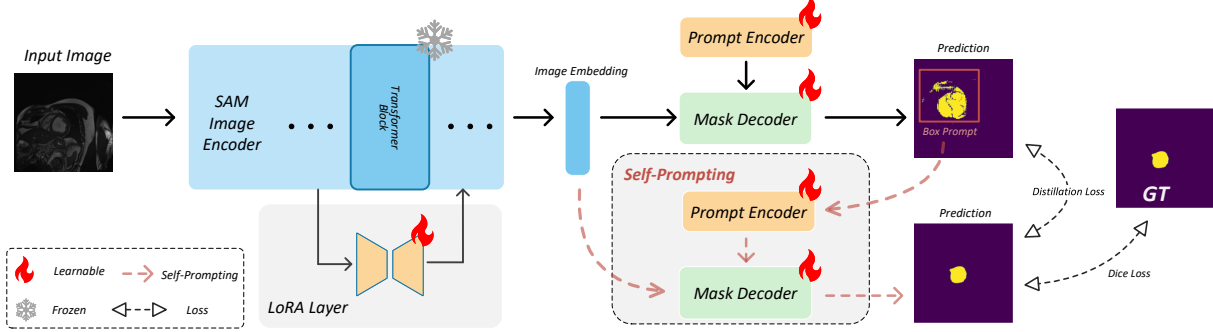


Figure 2: The overall training architecture of our proposed SAM-SP, which inherits from SAM and contains three additional modules: LoRA-based fine tuning, Self-Prompting module and Self-Distillation module. our proposed SAM-SP significantly enhance the segmentation capability of SAM in specific domains and alleviates the reliance on expert prompts during inference. The two prompt encoders here are shared with parameters, the same with two mask decoders.

an image  $x$ , we first obtain the image embedding  $E(x)$  via the image encoder  $E(\cdot)$  in SAM with LoRA. The vanilla prediction  $\hat{y}_0$  of our model without prompts is given by:

$$\hat{y}_0 = M(E(x), P(\text{none})) \quad (1)$$

To further alleviate the need of expert prompts, our model generates the prompts by itself without manual input. Specifically, we use the vanilla prediction  $\hat{y}_0$  from the first iteration to generate a prompt to guide the subsequent iteration. And a box prompt is produced using the maximum and minimum coordinates of the predicted mask  $\hat{y}_0$ , and we denote this self-prompting process as  $SP(\cdot)$ . Then, the prompt  $SP(\hat{y}_0)$  produced by the model itself is into the prompt encoder  $P(\cdot)$ , and the resulting self-prompt embedding  $P(SP(\hat{y}_0))$  combined with the image embedding  $E(x)$  is fed into the mask decoder  $M(\cdot)$ , formulated as:

$$\hat{y}_1 = M(E(x), P(SP(\hat{y}_0))) \quad (2)$$

where  $\hat{y}_1$  denotes the predicted result from the self-prompting process. This module enables the model to learn producing the prompts by itself, further reducing reliance on expert prompts.

Notably, the obtained image embeddings are used repeatedly during the self-prompting process, without adding obvious additional computational costs. And the introduced self-prompting module does not introduce any learnable parameters, keeping SAM-SP efficient.

### Self-Distillation Module

Inspired by the recent progresses in Knowledge Distillation (Gou et al. 2021; Wang and Yoon 2021), we utilize a segmentation based self-distillation module to further enhance the training of the self-prompting process. As mentioned earlier, we obtained the final predicted mask  $\hat{y}_1$  from the self-prompting process. Additionally, we also obtain the the vanilla predictions  $\hat{y}_0$  from our model. Specially, we employ the final prediction  $\hat{y}_1$  as the teacher to guide the previous prediction  $\hat{y}_0$  as the student. In this self-distillation module, SAM-SP gains mutual benefits from both the teacher

and student. The final prediction provides additional supervisory signals to guide the previous prediction. Simultaneously, the previous predictions help to refine the subsequent predictions by providing more accurate prompts. The self-distillation process is formulated as:  $L_{SD} = KL(\hat{y}_0, \hat{y}_1)$ , where  $L_{SD}$  denotes the knowledge distillation loss, with Kullback-Leibler Divergence as our default implementation.

Notably, the self-distillation module also does not introduce any learnable parameters and is deprecated during evaluation, further keeping SAM-SP efficient.

### Training and Evaluation

The overall training loss of SAM-SP is computed as:

$$L = Dice(\hat{y}_1, y) + \alpha L_{SD} \quad (3)$$

where  $y$  symbolizes the ground truth,  $Dice(\cdot)$  denotes Dice loss,  $\alpha$  serves as the weighting factor. Notably, our SAM-SP does not use any user-provided prompts during both training and inference.

## Experiments

In this section, we aim to validate the performance of our proposed SAM-SP model without the use of user-provided prompts during inference. To comprehensively assess the effectiveness of SAM-SP compared to state-of-the-art approaches, we conduct extensive experiments across 10 publicly available datasets.

### Benchmark Dataset

**Medical Image Segmentation.** Medical image segmentation is a critical and challenging task. In this evaluation, we select Polyp Segmentation (Jha et al. 2020) and Skin Lesion Segmentation (Berseth 2017) tasks. For Polyp Segmentation, we use 5 datasets: Kvasir-SEG (Jha et al. 2020), ClinicDB (Bernal et al. 2015), ColonDB (Tajbakhsh, Gurudu, and Liang 2015), Endoscene (Vázquez et al. 2017), and ETIS-LaribDB (Silva et al. 2014). Following previous settings (Fan et al. 2020), we adopt 900 and 548 images from

Table 1: Quantitative comparison on Polyp Segmentation of different approaches

Models	CVC-300		CVC-ClinicDB		Kvasir		ColonDB		ETIS-LaribDB	
	DICE	IoU								
U-Net (Ronneberger, Fischer, and Brox 2015)	71.0	62.7	82.3	75.5	81.8	74.6	51.2	44.4	39.8	33.5
UNet++ (Zhou et al. 2018)	70.7	62.4	79.4	72.9	82.1	74.3	48.3	41.0	40.1	34.4
PraNet (Fan et al. 2020)	87.1	79.7	89.9	84.9	89.8	84.0	71.2	64.0	62.8	56.7
UACANet-L (Kim, Lee, and Kim 2021)	88.21	80.84	91.07	86.7	90.83	85.95	72.57	65.41	63.89	56.87
SSFormerPVT (Wang et al. 2022)	<b>89.46</b>	<b>82.68</b>	92.88	88.27	91.11	86.01	79.34	70.63	78.03	70.1
PolypPVT (Dong et al. 2023)	88.71	81.89	<b>93.08</b>	<b>88.28</b>	<b>91.23</b>	<b>86.30</b>	<b>80.75</b>	<b>71.85</b>	<b>78.67</b>	<b>70.97</b>
SAM (Kirillov et al. 2023)	45.00	38.62	33.29	25.64	61.48	53.74	29.33	31.23	24.76	20.37
SAMed (Zhang and Liu 2023)	83.63	76.27	83.34	76.32	88.01	81.61	70.57	62.69	60.13	52.05
SAM-Med2D (Cheng et al. 2023)	84.81	77.49	85.91	80.60	87.06	80.88	69.08	60.79	59.80	53.00
Med-SA (Wu et al. 2023)	83.63	76.27	86.32	80.80	87.11	80.53	73.68	64.97	59.04	52.32
<b>SAM-SP (Ours)</b>	<b>88.94</b>	<b>82.55</b>	<b>85.91</b>	<b>80.37</b>	<b>90.57</b>	<b>85.46</b>	<b>74.67</b>	<b>67.24</b>	<b>64.87</b>	<b>58.11</b>

the ClinicDB and Kvasir datasets as the training set, and the remaining 64 and 100 images are employed as the respective test sets. To evaluate the generalization performance, we test the model on three unseen datasets: EndoScene, ColonDB and ETIS. For skin lesion segmentation, two skin lesion datasets are used: ISIC 2017 (Berseth 2017) with 2050 dermoscopy images, and ISIC 2018 (Codella et al. 2019) with 2694 dermoscopy images. To ensure a fair comparison, we follow the 7:3 train/test split strategy as outlined in (Ruan et al. 2023).

**Remote Sensing Images.** Remote sensing images (Zhang et al. 2020) typically cover a wide scope with complex backgrounds and diverse noise interference. ORSSD dataset (Li et al. 2019) contains 600 images for training and the rest 200 images for testing. EORSSD dataset (Zhang et al. 2020) is divided into two parts, where 1400 images for training and 600 images for testing.

**Distress detection.** Distress detection plays a crucial component in transportation infrastructure. We build a novel sub-grade distress detection dataset collected by an 3-Dimension ground penetrating radar (GPR) which is wildly employed in infrastructure health monitoring (Kim et al. 2021; Liu et al. 2021; Zhou et al. 2023a). This GPR dataset, named seg-GPR, consists of 395 images, with an 80/20 split for training and testing.

### Implementation Details and Baselines

We compare our proposed SAM-SP to several baselines, including task-specific segmentation approaches, the vanilla SAM, and SAM-based approaches. We re-implemented all SAM-base approaches using their open-source code, including SAM-Med2D (Cheng et al. 2023), Medical SAM Adapter (Med-SA) (Wu et al. 2023) and SAMed (Zhang and Liu 2023). For a fair comparison, these approaches are trained on the same training set of a dataset, and we uniformly use the ViT-B as the image encoder for SAM and SAM-based approaches. Our paper mainly focus the downstream performance without any use prompt. Consequently, no prompts are accessible for any approach during both training or inference periods, unless otherwise specified. We employ the AdamW optimizer (Loshchilov and Hutter 2019) in all experiments. For the learning rates and weight decays, we both make a gird search in the set  $\{1e-2, 1e-3, 1e-4, 1e-5\}$ .

Table 2: Quantitative comparison on Skin Lesion Segmentation of different approaches

Methods	ISIC2017		ISIC2018	
	DICE	IoU	DICE	IoU
U-Net	86.99	76.98	87.55	77.86
UNet++ (Zhou et al. 2018)	-	-	87.83	78.31
SANet (Wei et al. 2021)	-	-	88.59	79.52
TransFuse(Zhang, Liu, and Hu 2021)	88.40	79.21	89.27	80.63
MALUNet (Ruan et al. 2022)	88.13	78.78	89.04	80.25
EGE-Unet (Ruan et al. 2023)	<b>88.77</b>	79.81	89.04	80.25
SAM	53.28	40.80	58.79	46.06
SAM-Med2D	87.01	79.63	88.92	81.87
SAMed	85.86	77.51	88.73	79.84
Med-SA	87.78	80.35	88.75	81.77
<b>SAM-SP (Ours)</b>	<b>87.66</b>	<b>80.01</b>	<b>89.39</b>	<b>82.31</b>

Table 3: Quantitative comparison on Remote Sensing Images Segmentation of different approaches

Methods	ORSSD		EORSSD	
	DICE	IoU	DICE	IoU
DAFNet (Zhang et al. 2020)	87.4	82.3	83.0	80.0
MJRBm (Tu et al. 2021)	85.3	81.7	82.2	79.3
RRNet (Cong et al. 2021)	-	-	86.2	83.4
GateNet (Zhao et al. 2023b)	88.5	83.9	89.2	85.0
SAM	41.54	37.17	32.90	29.05
SAM-Med2D	89.38	83.19	88.13	81.68
SAMed	90.42	84.57	88.19	81.45
Med-SA	90.37	84.10	90.28	84.35
<b>SAM-SP (Ours)</b>	<b>92.66</b>	<b>87.53</b>	<b>91.01</b>	<b>85.22</b>

5}. Similarly, we search for the optimal number of training epochs of different approaches in the range  $\{100, 200, 300\}$ . Specially, we employ the warmup strategy (He et al. 2016) to stabilize the training process. Due our proposed SAM-SP is cost-effectiveness, SAM-SP can be run on a single NVIDIA RTX 3090 GPU. We use two wildly adopted evaluation metrics: Dice Similarity Coefficient (DICE) and Intersection over Union (IoU), defined as:  $Dice = \frac{2TP}{2TP + FP + FN}$  and  $IoU = \frac{TP}{TP + FP + FN}$ , respectively.

Table 4: Performance on Distress detection.

Methods	Seg-GPR	
	DICE	IoU
U-Net	66.23	54.87
SAM	20.89	11.28
SAMed	74.33	64.17
SAM-Med2D	72.95	62.46
<b>SAM-SP (Ours)</b>	<b>77.85</b>	<b>67.90</b>

Modules	ISIC2017		ISIC2018		ORSSD		Kvasir		Seg-GPR	
	DICE	IoU	DICE	IoU	DICE	IoU	DICE	IoU	DICE	IoU
vanilla SAM	53.28	40.80	58.79	46.06	41.54	37.17	61.48	53.74	20.89	11.28
+ LoRA	85.86	77.51	88.73	79.84	90.42	84.57	88.01	81.61	74.33	64.17
+ SP	87.03	79.69	89.17	81.96	92.25	86.99	89.95	84.56	77.32	67.20
+ KD (Ours)	87.66	80.01	89.39	82.31	92.66	87.53	90.57	85.46	77.85	67.99

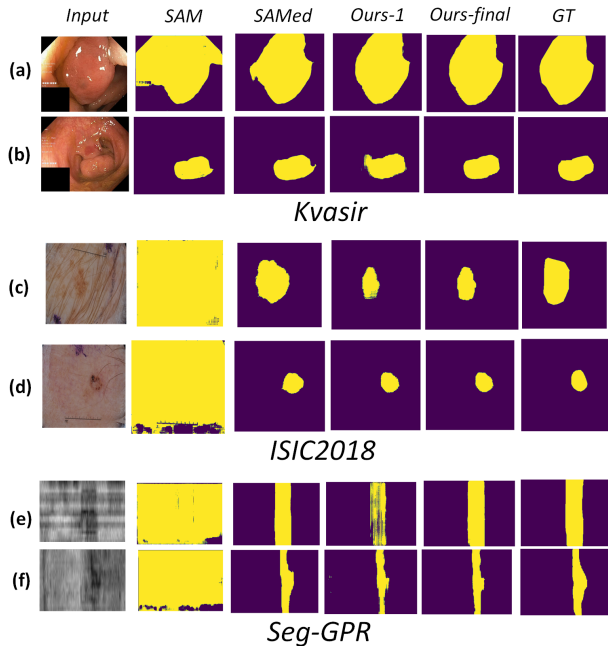


Figure 3: Visualization of segmentation results

## Main Results

**Quantitative results.** In Table 1, we summarize the qualitative results of our SAM-SP compared to other methods on the Polyp Segmentation task. Approaches in the top row are the task-specific segmentation approaches, and approaches in the middle row are SAM and SAM-based approaches. Specially, in our implementation, we provide user prompts for the vanilla SAM considering that it is a zero-shot Segmentation, following previous works (Wu et al. 2023). Here, SAM denotes the SAM with point prompts provided during inference, sampled within the ground-truth box. Similarly, Table 2, 3 and 4 summarize the quantitative results of our SAM-SP with other methods on Skin lesion segmentation, Remote Sensing Images Segmentation, Distress segmentation respectively. Firstly, observed from these quantitative results, our proposed SAM-SP achieve distinguished performance compared to the vanilla SAM and a series of SAM-based approaches across most downstream segmentation tasks, even without any prompts provided. For example, SAM-SP surpasses SAMMed2D with an obvious improvement on CVC-300, Kvasir, ColonDB and ETIS-LaribDB

Table 5: Ablation Studies on SAM-SP

datasets in the Polyp Segmentation task. Similarly, SAM-SP outperform SAMed with an obvious improvements on both the ISIC2018 and ISIC2017 datasets in the Skin lesion segmentation task. The similar performance improvements also be found on ORSSD, EORSSD and Seg-GPR Dataset. These improvements can be attributed to the our proposed self-prompting and self-distillation modules in SAM-SP, which enable the model to produce prompts autonomously, thus reducing reliance of user prompts during inference. Secondly, unfortunately, the vanilla SAM struggles to segment these domain-specific targets, and its performance is significantly lower than other SAM-based approaches. Though we provide the ground-truth based point prompts for SAM during inference, SAM still can not achieve the satisfied performances. Especially for our built Seg-GPR, it is a very challenging for the vanilla SAM, while our SAM-SP perform well in this dataset. Thirdly, our quantitative results also indicate that task-specific segmentation approaches still perform very competitively and, in some cases, still better than SAM-based approaches. For instance, while our proposed SAM-SP surpasses the state-of-the-art task-specific segmentation approaches in Skin lesion segmentation and Remote Sensing Images Segmentation tasks, it does not outperform the SOTA Polyp Segmentation tasks, such as SSFormerPVT and PolypPVT, which are specifically designed for the Polyp Segmentation with sophisticated network structures. How to allow Vision Foundation Models surpass the all SOTA task-specific approaches deserves further investigation.

**Qualitative results.** We showcase the qualitative results of our proposed SAM-SP in Figure 3 compared to the vanilla SAM and a SAM-based method SAMed. The top two rows show samples from Polyp Segmentation dataset, the middle two rows from the Skin lesion segmentation dataset, and the bottom two from the Seg-GPR dataset. Ours-1 denotes the first prediction of SAM-SP, and Ours-final means the final prediction of SAM-SP. These results indicate that, due to the absence of fine-tuning, the zero-shot SAM can not produce reliable segmentation results. Though SAMed achieves better segmentation results compared to the vanilla SAM, it still usually produce unclear boundary, as shown in 3(a). In contrast, our SAM-SP utilize the proposed self-prompting process to produce prompts autonomously, thus exhibiting more accurate predicted masks which closely resemble the ground truths in these samples from different datasets. Specially, we observe that our first output still performs competitively in some cases, which contributes to that our proposed

self-distillation module allow later prediction guide previous prediction. In summary, our proposed SAM-SP consistently performs well and produce satisfactory and high-quality segmentation results across various datasets, without relying on the user prompts during inference.

### Ablation Studies

As described earlier, our proposed SAM-SP inherits the basic structure of the vanilla SAM, and contains three additional modules: LoRA-based fine tuning, the self-prompting module, and the self-distillation module. Consequently, we investigate the effectiveness of each module in SAM-SP and summarize the experimental results in Table 5. These ablation results indicate that LoRA-based fine tuning (denoted as LoRA) provides the first performance boost compared to the vanilla SAM. The further performance boost occurs when the self-prompting module (denoted as SP) is introduced, which underscores its effectiveness. Finally, the employment of self-distillation module (denoted as KD) brings the additional performance gains, based on previous modules. The self-distillation module allows the previous and later prediction of SAM-SP gain benefits mutually. In summary, by coupling these three modules, SAM-SP achieves the satisfactory segmentation performance across various downstream datasets without relying on user-provided prompts.

### Model Analysis

**Self-Prompting Varieties** In our implementation of SAM-SP, we typically conduct the self-prompting process only once by default. Consequently, we investigate the impacts with multiple self-prompting processes in our proposed SAM-SP, and summaries experimental results with varying numbers of self-prompting processes in Figure 4. Firstly, observed from these results, the first self-prompting process brings the most significant performance boost compared to the second and third. Secondly, the more times of self-prompting processes may yield diminishing returns which may due to the convergence of output results in our self-prompting module. Therefore, for a balance between performance and efficiency, we default to a single self-prompting process in SAM-SP.

**Training Varieties** As described previously, our SAM-SP and other SAM-based approaches do not use any prompts during both training and testing phases, achieving consistency between training and testing conditions. To investigate whether the different prompt strategies during training affect the inference performance or not. Following previous works (Ma et al. 2024; Cheng et al. 2023), we conduct evaluations on Seg-GPR with different choices of prompt strategies during training, including: no prompt (None), Ground-truth Random Point Prompt (Randompoint) and Ground-truth Center Point Prompt (GTpoint). Notably, we still ensure that no prompts are provided during inference. As summarized in Fig 5, SAM-SP, along with other SAM-based approaches, performs best when no prompts are used during training, compared to other training prompt strategies. Interestingly, although GTpoint provides more accurate ground-truth information, it leads to worse inference performance.

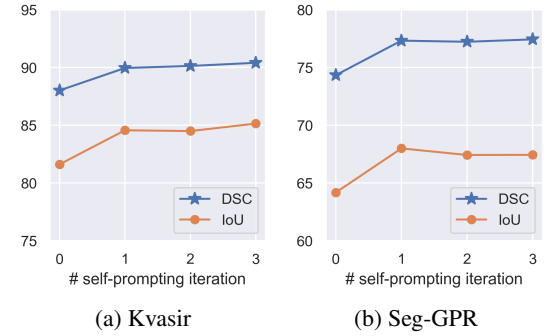


Figure 4: Quantitative comparison with different number of self-prompting iterations.

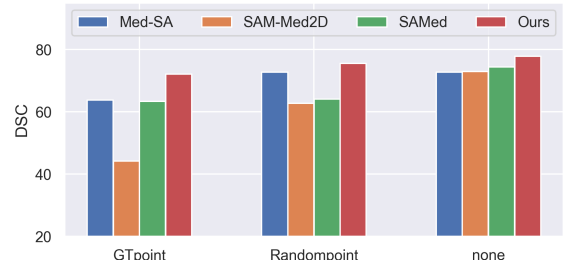


Figure 5: Comparison with different training strategies.

This counter-intuitive results may be due to that accurate prompts provided during training makes the model overly reliant on provided prompts, thus leading to significant performance degradation when no prompts are available during inference. Additionally, the use of GTpoint prompts severely degrades the inference performance of SAM-Med2D. On the contrary, our SAM-SP experience only minor performance changes with GTpoint prompts. This may be attributed to our proposed self-prompting module, which endeavor to produce reliable prompts autonomously, reducing reliance on externally provided prompts.

### Conclusion

In this paper, we first emphasize the significance of reducing reliance on expert prompts when applying visual foundation models to specific domains, such as the Segment Anything Model (SAM), which broadens the application range of models. To alleviate the need for expert prompts in various specific domains, we introduce a novel self-prompting based fine-tuning approach SAM-SP, tailored for extending the capabilities of the vanilla SAM model. Specifically, SAM-SP leverages its own output from the previous iteration as prompts to guide the subsequent iteration of the model. This self-prompting module endeavors to learn how to generate effective prompts autonomously and alleviates the dependency on expert prompts during evaluation, significantly broadening SAM’s applicability. Additionally, we integrate a self-distillation module to further enhance the self-prompting process. Extensive experiments across vari-

ous datasets validate the effectiveness of the proposed SAM-SP, which not only alleviates the reliance on expert prompts but also exhibits satisfactory performance. We hope that our study will benefit future research in self-prompting, and help reduce the dependence on expert prompts when applying visual foundation models to specific domains.

## References

Achiam, J.; Adler, S.; Agarwal, S.; Ahmad, L.; Akkaya, I.; Aleman, F. L.; Almeida, D.; Altenschmidt, J.; Altman, S.; Anadkat, S.; et al. 2023. GPT-4 technical report. *arXiv preprint arXiv:2303.08774*.

Ahmadi, M.; Lonbar, A. G.; Sharifi, A.; Beris, A. T.; Nouri, M.; and Javidi, A. S. 2023. Application of Segment Anything Model for Civil Infrastructure Defect Assessment. *arXiv:2304.12600*.

Bernal, J.; Sánchez, F. J.; Fernández-Esparrach, G.; Gil, D.; Rodríguez, C.; and Vilariño, F. 2015. WM-DOVA maps for accurate polyp highlighting in colonoscopy: Validation vs. saliency maps from physicians. *Computerized medical imaging and graphics*, 43: 99–111.

Berseth, M. 2017. ISIC 2017-skin lesion analysis towards melanoma detection. *arXiv preprint arXiv:1703.00523*.

Bommasani, R.; Hudson, D. A.; Adeli, E.; Altman, R.; Arora, S.; von Arx, S.; Bernstein, M. S.; Bohg, J.; Bosselut, A.; Brunskill, E.; et al. 2021. On the opportunities and risks of foundation models. *arXiv preprint arXiv:2108.07258*.

Chen, S.; Ge, C.; Tong, Z.; Wang, J.; Song, Y.; Wang, J.; and Luo, P. 2022. Adaptformer: Adapting vision transformers for scalable visual recognition. *Advances in Neural Information Processing Systems*, 35: 16664–16678.

Chen, T.; Zhu, L.; Ding, C.; Cao, R.; Wang, Y.; Li, Z.; Sun, L.; Mao, P.; and Zang, Y. 2023. SAM fails to segment anything?—SAM-adapter: Adapting SAM in underperformed scenes: Camouflage, shadow, medical image segmentation, and more. *arXiv preprint arXiv:2304.09148*.

Cheng, J.; Ye, J.; Deng, Z.; Chen, J.; Li, T.; Wang, H.; Su, Y.; Huang, Z.; Chen, J.; Jiang, L.; et al. 2023. Sam-med2d. *arXiv preprint arXiv:2308.16184*.

Codella, N.; Rotemberg, V.; Tschandl, P.; Celebi, M. E.; Dusza, S.; Gutman, D.; Helba, B.; Kalloo, A.; Liopyris, K.; Marchetti, M.; et al. 2019. Skin lesion analysis toward melanoma detection 2018: A challenge hosted by the international skin imaging collaboration (isic). *arXiv preprint arXiv:1902.03368*.

Cong, R.; Zhang, Y.; Fang, L.; Li, J.; Zhao, Y.; and Kwong, S. 2021. RRNet: Relational reasoning network with parallel multiscale attention for salient object detection in optical remote sensing images. *IEEE Transactions on Geoscience and Remote Sensing*, 60: 1–11.

Dong, B.; Wang, W.; Fan, D.-P.; Li, J.; Fu, H.; and Shao, L. 2023. Polyp-PVT: Polyp Segmentation with Pyramid Vision Transformers. *CAAI Artificial Intelligence Research*, 2.

Dosovitskiy, A.; Beyer, L.; Kolesnikov, A.; Weissenborn, D.; Zhai, X.; Unterthiner, T.; Dehghani, M.; Minderer, M.; Heigold, G.; Gelly, S.; et al. 2020. An image is worth 16x16 words: Transformers for image recognition at scale. *arXiv preprint arXiv:2010.11929*.

Fan, D.-P.; Ji, G.-P.; Zhou, T.; Chen, G.; Fu, H.; Shen, J.; and Shao, L. 2020. Pranet: Parallel reverse attention network for polyp segmentation. In *International conference on medical image computing and computer-assisted intervention*, 263–273. Springer.

Fan, R.; Bocus, M. J.; Zhu, Y.; Jiao, J.; Wang, L.; Ma, F.; Cheng, S.; and Liu, M. 2019. Road Crack Detection Using Deep Convolutional Neural Network and Adaptive Thresholding. *2019 IEEE Intelligent Vehicles Symposium (IV)*, 474–479.

Gou, J.; Yu, B.; Maybank, S. J.; and Tao, D. 2021. Knowledge distillation: A survey. *International Journal of Computer Vision*, 129(6): 1789–1819.

He, K.; Chen, X.; Xie, S.; Li, Y.; Dollár, P.; and Girshick, R. 2022. Masked autoencoders are scalable vision learners. In *Proceedings of the IEEE/CVF conference on computer vision and pattern recognition*, 16000–16009.

He, K.; Zhang, X.; Ren, S.; and Sun, J. 2016. Deep residual learning for image recognition. In *Proceedings of the IEEE conference on computer vision and pattern recognition*, 770–778.

He, S.; Bao, R.; Li, J.; Stout, J.; Bjornerud, A.; Grant, P. E.; and Ou, Y. 2023. Computer-Vision Benchmark Segment-Anything Model (SAM) in Medical Images: Accuracy in 12 Datasets. *arXiv:2304.09324*.

Hesamian, M. H.; Jia, W.; He, X.; and Kennedy, P. J. 2019. Deep Learning Techniques for Medical Image Segmentation: Achievements and Challenges. *Journal of Digital Imaging*, 32: 582 – 596.

Hu, E. J.; Wallis, P.; Allen-Zhu, Z.; Li, Y.; Wang, S.; Wang, L.; Chen, W.; et al. 2021. LoRA: Low-Rank Adaptation of Large Language Models. In *International Conference on Learning Representations*.

Jha, D.; Smedsrød, P. H.; Riegler, M. A.; Halvorsen, P.; De Lange, T.; Johansen, D.; and Johansen, H. D. 2020. Kvasir-seg: A segmented polyp dataset. In *MultiMedia Modeling: 26th International Conference, MMM 2020, Daejeon, South Korea, January 5–8, 2020, Proceedings, Part II* 26, 451–462. Springer.

Ji, W.; Li, J.; Bi, Q.; Li, W.; and Cheng, L. 2023. Segment anything is not always perfect: An investigation of sam on different real-world applications. *arXiv preprint arXiv:2304.05750*.

Jiang, H.; Peng, M.; Zhong, Y.; Xie, H.; Hao, Z.; Lin, J.; Ma, X.; and Hu, X. 2022. A Survey on Deep Learning-Based Change Detection from High-Resolution Remote Sensing Images. *Remote. Sens.*, 14: 1552.

Kenton, J. D. M.-W. C.; and Toutanova, L. K. 2019. BERT: Pre-training of Deep Bidirectional Transformers for Language Understanding. In *Proceedings of NAACL-HLT*, 4171–4186.

Kim, N.; Kim, S.; An, Y.-K.; and Lee, J.-J. 2021. A novel 3D GPR image arrangement for deep learning-based underground object classification. *International Journal of Pavement Engineering*, 22(6): 740–751.

Kim, T.; Lee, H.; and Kim, D. 2021. Uacanet: Uncertainty augmented context attention for polyp segmentation. In *Proceedings of the 29th ACM international conference on multimedia*, 2167–2175.

Kirillov, A.; Mintun, E.; Ravi, N.; Mao, H.; Rolland, C.; Gustafson, L.; Xiao, T.; Whitehead, S.; Berg, A. C.; Lo, W.-Y.; et al. 2023. Segment anything. In *Proceedings of the IEEE/CVF International Conference on Computer Vision*, 4015–4026.

Li, C.; Cong, R.; Hou, J.; Zhang, S.; Qian, Y.; and Kwong, S. 2019. Nested network with two-stream pyramid for salient object detection in optical remote sensing images. *IEEE Transactions on Geoscience and Remote Sensing*, 57(11): 9156–9166.

Li, J.; Li, D.; Xiong, C.; and Hoi, S. 2022. Blip: Bootstrapping language-image pre-training for unified vision-language understanding and generation. In *International conference on machine learning*, 12888–12900. PMLR.

Lin, X.; Xiang, Y.; Zhang, L.; Yang, X.; Yan, Z.; and Yu, L. 2023. Samus: Adapting segment anything model for clinically-friendly and generalizable ultrasound image segmentation. *arXiv preprint arXiv:2309.06824*.

Litjens, G. J. S.; Kooi, T.; Bejnordi, B. E.; Setio, A. A. A.; Ciompi, F.; Ghafoorian, M.; van der Laak, J.; van Ginneken, B.; and Sánchez, C. I. 2017. A survey on deep learning in medical image analysis. *Medical image analysis*, 42: 60–88.

Liu, Z.; Wu, W.; Gu, X.; Li, S.; Wang, L.; and Zhang, T. 2021. Application of combining YOLO models and 3D GPR images in road detection and maintenance. *Remote Sensing*, 13(6): 1081.

Loshchilov, I.; and Hutter, F. 2019. Decoupled Weight Decay Regularization. *arXiv:1711.05101*.

Ma, J.; He, Y.; Li, F.; Han, L.; You, C.; and Wang, B. 2024. Segment anything in medical images. *Nature Communications*, 15(1): 654.

Mattjie, C.; De Moura, L. V.; Ravazio, R. C.; Kupssinskü, L. S.; Parraga, O.; Delucis, M. M.; and Barros, R. C. 2023. Zero-shot performance of the Segment Anything Model (SAM) in 2D medical imaging: A comprehensive evaluation and practical guidelines. *arXiv preprint arXiv:2305.00109*.

Minaee, S.; Boykov, Y.; Porikli, F.; Plaza, A.; Kehtarnavaz, N.; and Terzopoulos, D. 2021. Image segmentation using deep learning: A survey. *IEEE transactions on pattern analysis and machine intelligence*, 44(7): 3523–3542.

Ning, K.; Zhou, C.; and Yu, Z. 2023. Segment anything model for subgrade distress detection with GPR. In *2023 IEEE 3rd International Conference on Data Science and Computer Application (ICDSCA)*, 122–127. IEEE.

Ouyang, L.; Wu, J.; Jiang, X.; Almeida, D.; Wainwright, C.; Mishkin, P.; Zhang, C.; Agarwal, S.; Slama, K.; Ray, A.; et al. 2022. Training language models to follow instructions with human feedback. *Advances in neural information processing systems*, 35: 27730–27744.

Radford, A.; Kim, J. W.; Hallacy, C.; Ramesh, A.; Goh, G.; Agarwal, S.; Sastry, G.; Askell, A.; Mishkin, P.; Clark, J.; et al. 2021. Learning transferable visual models from natural language supervision. In *International conference on machine learning*, 8748–8763. PMLR.

Ramesh, A.; Pavlov, M.; Goh, G.; Gray, S.; Voss, C.; Radford, A.; Chen, M.; and Sutskever, I. 2021. Zero-shot text-to-image generation. In *International conference on machine learning*, 8821–8831. PMLR.

Ronneberger, O.; Fischer, P.; and Brox, T. 2015. U-net: Convolutional networks for biomedical image segmentation. In *Medical image computing and computer-assisted intervention–MICCAI 2015: 18th international conference, Munich, Germany, October 5–9, 2015, proceedings, part III* 18, 234–241. Springer.

Ruan, J.; Xiang, S.; Xie, M.; Liu, T.; and Fu, Y. 2022. MALUNet: A multi-attention and light-weight unet for skin lesion segmentation. In *2022 IEEE International Conference on Bioinformatics and Biomedicine (BIBM)*, 1150–1156. IEEE.

Ruan, J.; Xie, M.; Gao, J.; Liu, T.; and Fu, Y. 2023. Ege-unet: an efficient group enhanced unet for skin lesion segmentation. In *International Conference on Medical Image Computing and Computer-Assisted Intervention*, 481–490. Springer.

Shafique, A.; Cao, G.; Khan, Z.; Asad, M.; and Aslam, M. 2022. Deep Learning-Based Change Detection in Remote Sensing Images: A Review. *Remote. Sens.*, 14: 871.

Silva, J.; Histace, A.; Romain, O.; Dray, X.; and Granado, B. 2014. Toward embedded detection of polyps in wce images for early diagnosis of colorectal cancer. *International journal of computer assisted radiology and surgery*, 9: 283–293.

Tajbakhsh, N.; Gurudu, S. R.; and Liang, J. 2015. Automated polyp detection in colonoscopy videos using shape and context information. *IEEE transactions on medical imaging*, 35(2): 630–644.

Tu, Z.; Wang, C.; Li, C.; Fan, M.; Zhao, H.; and Luo, B. 2021. ORSI salient object detection via multiscale joint region and boundary model. *IEEE Transactions on Geoscience and Remote Sensing*, 60: 1–13.

Vázquez, D.; Bernal, J.; Sánchez, F. J.; Fernández-Esparrach, G.; López, A. M.; Romero, A.; Drozdal, M.; and Courville, A. 2017. A benchmark for endoluminal scene segmentation of colonoscopy images. *Journal of healthcare engineering*, 2017.

Wang, J.; Huang, Q.; Tang, F.; Meng, J.; Su, J.; and Song, S. 2022. Stepwise feature fusion: Local guides global. In *International Conference on Medical Image Computing and Computer-Assisted Intervention*, 110–120. Springer.

Wang, L.; and Yoon, K.-J. 2021. Knowledge distillation and student-teacher learning for visual intelligence: A review and new outlooks. *IEEE transactions on pattern analysis and machine intelligence*, 44(6): 3048–3068.

Wei, J.; Hu, Y.; Zhang, R.; Li, Z.; Zhou, S. K.; and Cui, S. 2021. Shallow attention network for polyp segmentation. In *Medical Image Computing and Computer Assisted Intervention–MICCAI 2021: 24th International Conference, Strasbourg, France, September 27–October 1, 2021, Proceedings, Part I* 24, 699–708. Springer.

Wu, J.; Fu, R.; Fang, H.; Liu, Y.; Wang, Z.; Xu, Y.; Jin, Y.; and Arbel, T. 2023. Medical sam adapter: Adapting segment anything model for medical image segmentation. *arXiv preprint arXiv:2304.12620*.

Wu, Q.; Zhang, Y.; and Elbatel, M. 2023. Self-prompting large vision models for few-shot medical image segmentation. In *MICCAI workshop on domain adaptation and representation transfer*, 156–167. Springer.

Yang, X.; Li, X.; Ye, Y.; Lau, R. Y. K.; Zhang, X.; and Huang, X. 2019. Road Detection and Centerline Extraction Via Deep Recurrent Convolutional Neural Network U-Net. *IEEE Transactions on Geoscience and Remote Sensing*, 57: 7209–7220.

Zhang, K.; and Liu, D. 2023. Customized segment anything model for medical image segmentation. *arXiv preprint arXiv:2304.13785*.

Zhang, Q.; Cong, R.; Li, C.; Cheng, M.-M.; Fang, Y.; Cao, X.; Zhao, Y.; and Kwong, S. 2020. Dense attention fluid network for salient object detection in optical remote sensing images. *IEEE Transactions on Image Processing*, 30: 1305–1317.

Zhang, Y.; Liu, H.; and Hu, Q. 2021. Transfuse: Fusing transformers and cnns for medical image segmentation. In *Medical Image Computing and Computer Assisted Intervention—MICCAI 2021: 24th International Conference, Strasbourg, France, September 27–October 1, 2021, Proceedings, Part I* 24, 14–24. Springer.

Zhao, W. X.; Zhou, K.; Li, J.; Tang, T.; Wang, X.; Hou, Y.; Min, Y.; Zhang, B.; Zhang, J.; Dong, Z.; et al. 2023a. A survey of large language models. *arXiv preprint arXiv:2303.18223*.

Zhao, X.; Pang, Y.; Zhang, L.; Lu, H.; and Zhang, L. 2023b. Towards diverse binary segmentation via a simple yet general gated network. *arXiv preprint arXiv:2303.10396*.

Zhou, C.; Ning, K.; Wang, H.; Yu, Z.; Zhou, S.; and Bu, J. 2023a. Multi-View Fusion and Distillation for Subgrade Distresses Detection based on 3D-GPR. *arXiv preprint arXiv:2308.04779*.

Zhou, T.; Zhang, Y.; Zhou, Y.; Wu, Y.; and Gong, C. 2023b. Can sam segment polyps? *arXiv preprint arXiv:2304.07583*.

Zhou, Z.; Rahman Siddiquee, M. M.; Tajbakhsh, N.; and Liang, J. 2018. Unet++: A nested u-net architecture for medical image segmentation. In *Deep Learning in Medical Image Analysis and Multimodal Learning for Clinical Decision Support: 4th International Workshop, DLMIA 2018, and 8th International Workshop, ML-CDS 2018, Held in Conjunction with MICCAI 2018, Granada, Spain, September 20, 2018, Proceedings* 4, 3–11. Springer.

Zhou, Z.; Siddiquee, M. M. R.; Tajbakhsh, N.; and Liang, J. 2020. UNet++: Redesigning Skip Connections to Exploit Multiscale Features in Image Segmentation. *IEEE Transactions on Medical Imaging*, 39(6): 1856–1867.